

## N O T I C E

THIS DOCUMENT HAS BEEN REPRODUCED FROM  
MICROFICHE. ALTHOUGH IT IS RECOGNIZED THAT  
CERTAIN PORTIONS ARE ILLEGIBLE, IT IS BEING RELEASED  
IN THE INTEREST OF MAKING AVAILABLE AS MUCH  
INFORMATION AS POSSIBLE

MS

NASA Technical Memorandum 82828

# Correlation of Tensile and Shear Strengths of Metals With Their Friction Properties

(NASA-TM-82828) CORRELATION OF TENSILE AND SHEAR STRENGTHS OF METALS WITH THEIR FRICTION PROPERTIES (NASA) 23 p  
HC A02/MF A01

N82-24325

CSCL 11F

Unclas

G3/26 09982

Kazuhisa Miyoshi and Donald H. Buckley  
*Lewis Research Center*  
*Cleveland, Ohio*



Prepared for the  
Joint Lubrication Conference  
cosponsored by the American Society of Mechanical Engineers  
and the American Society of Lubrication Engineers  
Washington, D.C., October 5-7, 1982



# CORRELATION OF TENSILE AND SHEAR STRENGTHS OF METALS WITH THEIR FRICTION PROPERTIES

by Kazuhisa Miyoshi and Donald H. Buckley  
National Aeronautics and Space Administration  
Lewis Research Center  
Cleveland, Ohio 44135

## ABSTRACT

The relation between the theoretical tensile and the shear strengths and the friction properties of metals in contact with diamond, boron nitride, silicon carbide, manganese-zinc ferrite, and the metals themselves in vacuum was investigated. The relationship between the actual shear strength and the friction properties of the metal was also investigated. An estimate of the theoretical uniaxial tensile strength was obtained in terms of the equilibrium surface energy, interplanar spacing of the planes perpendicular to the tensile axis, and the Young's modulus of elasticity. An estimate of the theoretical shear strength for metals was obtained from the shear modulus, the repeat distance of atoms in the direction of shear of the metal and the interplanar spacing of the shear planes. The coefficient of friction for metals was found to be related to the theoretical tensile, theoretical shear, and actual shear strengths of metals. The higher the strength of the metal, the lower the coefficient of friction.

## INTRODUCTION

In the 1940's Pauling recognized differences in the amount of the d-bond character associated with transition metals (ref. 1). Since the d-valence bands are not completely filled in the transition metals, the filling of the d-valence electron band in transition metals is responsible for such physical and chemical properties as cohesive energy, shear modulus, chemical stability, and magnetic properties. The greater the amount or the

percentage of d-bond character that a metal possesses, the less active is its surface. The adhesion and friction of metals in contact with themselves can be related to the chemical activity of the metal surfaces (ref. 2). The d-bond character of the metal influences the adhesion and friction for metals in contact with diamond, pyrolytic boron nitride, silicon carbide, and manganese-zinc ferrite crystals, just as it does for metals in contact with themselves (refs. 3 to 6). The more active the metal, the higher the coefficient of friction.

It should, however, also be possible to determine such tribological properties as friction in terms of the physical and mechanical properties of these metals as well.

The objective of this paper was to investigate the relationship between the theoretical tensile strength, theoretical shear strength, and actual shear strengths with the friction properties of metals when those metals are in contact with metals and nonmetals.

As greater and greater mechanical strengths are obtained from engineering materials, it is only logical to ask, What is the upper limit to the strength of a solid? This upper limit or maximum strength has come to be referred to as the theoretical strength.

An estimate of the theoretical (ideal) uniaxial tensile strength  $\sigma_{\max}$  for metals was obtained from equilibrium surface energy and interplanar spacing of the planes perpendicular to the tensile axis, and the Young's modulus of elasticity. The theoretical shear strength  $\tau_{\max}$  of a solid subjected to a simple shear mode of deformation is estimated (ref. 7). The actual shear strengths for the metals are taken from the data of Bridgman (ref. 8).

Coefficients of friction for various pure elemental metals in contact with diamond, pyrolytic boron nitride, silicon carbide, manganese-zinc ferrite, and the metals themselves were taken from our previous studies (refs. 2 to 6). Some additional data were taken from the experiments, which were conducted in the same manner as reported earlier in references 2 to 6.

In references 2 to 6, all sliding friction experiments were conducted with light loads, 0.01 to 0.5 newton, at a sliding velocity 0.70, 0.77, or 3 millimeter per minute, in a high vacuum of  $3 \times 10^{-8}$  pascal and at room temperature. Frictional heating did not produce a measurable temperature rise. Experiments were conducted in this investigation with the metal pin specimens sliding on the metal or nonmetal flats. The radius of pin specimen was 0.79 millimeter.

#### SYMBOLS

b	repeat distance of atoms in the direction of shear
d	interplanar spacing of shearing planes
E	Young's modulus
$\bar{F}_{\max}$	average friction force
G	shear modulus
k	constant
W	normal load
x	displacement of the shear plane from its neighbors
$\gamma$	surface energy per unit area
$\mu$	coefficient of friction
$\sigma_{\max}$	theoretical tensile strength
$\tau_{\max}$	theoretical shear strength

## THEORETICAL STRENGTH OF SOLIDS

The generally accepted thinking with respect to the fracture of solids is that the ideal elastic solid is one which exhibits elastic response to a load until such time as atomic separation takes place on a plane by overcoming the interatomic forces. At the atomistic level fracture occurs when bonds between atoms are broken across a fracture plane and a new surface is created. This can occur by breaking bonds perpendicular to the fracture plane (fig. 1(a)) or by shearing bonds across the fracture plane (fig. 1(b)). Such behavior is expected in the case of an ideal crystalline solid which contains no defects. Under such conditions criteria for fracture are simple; fracture occurs when the local stress builds up either to the theoretical cohesive strength or to the theoretical shear strength.

The calculation of the theoretical cohesive strength of an ideal elastic solid is based on the proposition that all the energy used in separation is available for the creation of two new surfaces with the only expenditure of energy in creating these two surfaces is assumed to be the surface energy. If the atoms A and A' in figure 1(a) are pulled apart, the stress required to separate the plane is the theoretical strength  $\sigma_{\max}$  and when that is reached, the bonds are broken. The theoretical strength (the theoretical uniaxial tensile strength) is then given by well-known equation,

$$\sigma_{\max} = \sqrt{\frac{E\gamma}{d}} \quad (1)$$

where E is the appropriate Young's modulus,  $\gamma$  is the surface energy per unit area, and d is the interplanar spacing of the planes perpendicular to the tensile axis (refs. 7 or 9 to 12). In the equation the theoretical strength of solid is directly related to other macroscopic physical properties. The foregoing approach is equally applicable to any solid. Frenkel

used a similar method to estimate the theoretical shear strength  $\tau_{\max}$  of a solid subjected to a simple shear mode of deformation (ref. 7 or 13). It is assumed that, for any solid, the stress to shear any plane a distance  $x$  over its neighbor is given by

$$\tau = k \sin \frac{2\pi x}{b} \quad (2)$$

where  $b$  is the appropriate repeat distance in the direction of shear (the planes are assumed to be undistorted by the shear) and  $k$  is chosen to give the correct shear modulus  $G$ . It is then easily shown that

$$\tau_{\max} = \frac{Gb}{2\pi d} \quad (3)$$

where  $d$  is the interplanar spacing of the shearing planes.

#### PHYSICAL PROPERTIES

Surface energies of solid metals have been reported in the literature (refs. 14 to 21). Table I is a compilation of surface energy values by Tyson and Miedema (refs. 14 and 21). Miedema (ref. 21) estimated values at absolute zero temperature  $\gamma_0^S$  from values of the experimental surface energy and entropy. Values at room temperature of  $\gamma^S$  were calculated using the values of  $\gamma_0^S$  and the temperature dependence factors estimated by Miedema.

The surface energy data referred to herein are mean values. Anisotropy of the surface energy is not considered in this paper (although it may be remarked that while anisotropy exists it is usually small, with variations from the average of the order of 10 percent for example for cubic metals (refs. 22 and 24). Table I lists elastic moduli  $E$  and lattice constants for the metals used in this paper (from refs. 25 to 27). Young's modulus is for bulk, polycrystalline materials.

The values of the shear moduli for bulk, polycrystalline materials are listed in table I (ref. 25). The shear modulus, like Young's modulus, has a marked dependence on the electronic configuration of the element (ref. 25). The values of the lattice constants are used for the estimations of an interplanar spacing of slip plane and an atomic spacing in the direction of shear. The experimental results of slip systems at room temperature are given in table I (ref. 28).

## RESULTS AND DISCUSSION

### Correlation of Coefficient of Friction with Theoretical Tensile Strength

A clean metal in sliding contact with a clean nonmetal or the metal itself will fail either in tension or in shear because some of the interfacial bonds are generally stronger than the cohesive bonds in the cohesively weaker metal. The failed metal subsequently transfers to nonmetallic material or the other contacting metal (see fig. 2 and refs. 2 to 6). It is, therefore, anticipated that friction, metal transfer, and metal wear would be related to chemical, physical, and metallurgical properties and to the strength of metals. Therefore, let us consider the relation between the theoretical tensile strength and the tribological properties.

The values of the theoretical tensile strength obtained from equation (1) are presented in table II. The values of the coefficient of friction for various pure elemental metals in contact with diamond (ref. 3), pyrolytic boron nitride (ref. 4), silicon carbide (ref. 5), manganese-zinc ferrite (ref. 6), and the metals themselves (ref. 2) are presented in table III.

Figure 3 presents the coefficients of friction as a function of  $\sigma_{\max}$ . The data of these figures indicate a decrease in friction with an increase of the theoretical tensile strength of the metal bond. There generally

appears to be a strong correlation between friction and the theoretical tensile strength of metals. The higher the tensile strength, the lower the friction.

On separation of the metallic and nonmetallic material in sliding contact, fracture occurs in the metal as well as the shearing at the adhesive bonds in the interface. The morphology of metal transfer to the nonmetal revealed that the metals that have low tensile strength exhibit much more transfer than those that have higher tensile strength.

For example, examination of wear tracks on the silicon carbide after single pass sliding with titanium revealed evidence of both very thin transfer films and lump particles of titanium transferred to the silicon carbide. On the other hand, examination of the silicon carbide surface after multipass sliding with titanium indicated the presence of very thin transfer films, multilayer transfer films, very small particles, and pile up of particles. Table IV summarizes metal transfer to single-crystal silicon carbide observed after multiple passes sliding. Generally, metals farther to the right in table IV have less chemical affinity for silicon and carbon and greater resistance to tensile and shear fracture, and accordingly lower coefficients of friction. Therefore, with metals further to the right in table IV, less transfer to silicon carbide was observed.

Such dependency of metal transfer on the theoretical tensile strength arises from the adhesion and fracture properties of the metal. Thus, the theoretical tensile strengths which are functions of the surface energy, Young's modulus, and interplanar spacing in the crystal, play roles in the adhesion and friction and transfer of metals contacting metals or nonmetals.

Further correlations between surface energy and other physical properties have been sought by many investigators (refs. 14, 15 and 21). The most

successful and widely accepted of these correlations for elemental solids occurs where the heat of sublimation has been considered. A good correlation between surface and cohesive energy was also, however, found by Tyson and Jones (refs. 14 and 15).

#### Correlation of Coefficient of Friction with Theoretical Shear Strength

From equation (3) the values of the theoretical shear strength were obtained and these are presented in table V. It is assumed that the slip occurred on the slip plane in the slip direction, as indicated in table V.

Figure 4 presents the coefficients of friction as a function of the theoretical shear strength. These figures indicate a decrease in friction with an increase in the theoretical shear strength of the metal bond.

The theoretical shear strength generally produces a correlation with the coefficients of friction for metals in contact with such nonmetals as diamond, pyrolytic boron nitride, silicon carbide, and manganese-zinc ferrite, as shown in figure 4. The coefficients of friction for metals in contact with themselves correlate with the metal shear strength, except for platinum and palladium, as indicated in figure 4. In these figures the values of the shear strength for face-centered cubic metals are used from the results shown in table V.

The shear strength values for the body-centered cubic metals are average values calculated from the values of the shear strength for three dominant slip systems. Those for the hexagonal metals are average values calculated from the shear strengths for two dominant slip systems, that is, the  $\{10\bar{1}0\}$ ,  $\langle 11\bar{2}0 \rangle$  and  $\{0001\} \langle 11\bar{2}0 \rangle$ .

Thus, the tensile and shear properties play important roles in the adhesion and friction of metals contacting nonmetals or metals contacting themselves. These simple calculations of the theoretical strength and the

correlation between the friction and the strength can be criticized on a variety of grounds. The extent of slip in a crystal depends on the magnitude of the shearing stresses produced by the applied forces and the orientation of the crystal with respect to these applied forces. This variation can be rationalized by the concept of the crystal's resolved shear stress for slip. Despite the foregoing the results of the relation between the coefficient of friction and the theoretical strength may lead in turn to an appreciation for the role of the physical properties of materials in determining the tribological properties and the mechanical behavior of metals.

A good correlation between the coefficients of friction and the shear modulus (refer to table V) was also found with metals contacting nonmetals. The correlations are very similar to those between the coefficient of friction and the shear strength, as shown in figure 4. This is to be expected at least for face-centered cubic and close-packed hexagonal metals because, as shown in table V, the ratios of  $\tau_{\max}$  to G are essentially constant at a value of about 0.1. With the body centered cubic metals the ratio of  $\tau_{\max}/G$  is essentially constant at a value of about 0.6.

#### Correlation of Coefficient of Friction with Actual Shear Strength

The theoretical shear strength as well as the theoretical tensile strength are much greater than the values commonly found experimentally. In the former sections the relationships between the theoretical strengths and the friction properties of metals in contact with nonmetals and the metals with themselves were discussed. There is, however, an obvious need to compare the actual strength of metals observed with the friction properties.

The actual shear strengths of metals were estimated from the experimental data of Bridgman (ref. 8). The shear phenomena and strength combined with high hydrostatic pressure were studied at pressures to a maximum of 4.9

gigapascals. The shear strength of the metal is very strongly dependent on the hydrostatic pressure acting on the specimen during the shearing process. The shear strength of the metal is increased with increasing applied hydrostatic pressure. The shear strength was estimated by extrapolation from contact pressure during sliding experiments by using the relations between the hydrostatic pressure and the shear strength obtained by Bridgman (ref. 8). The contact pressures for various metals in contact with non-metals are calculated with Hertz's classical equations (ref. 29).

Figure 5 represents the friction properties of metals in contact with clean diamond, silicon carbide, and manganese-zinc ferrite as functions of the actual shear strength. The data of these figures indicate a decrease in friction with an increase of the actual shear strength of metal. There generally appears to be correlation between the friction and the actual shear strength of metal. This seems to indicate that the ratio of actual to theoretical shear strength does not vary greatly from one elemental metal to another.

#### SUMMARY OF RESULTS

An estimate of the theoretical uniaxial tensile strength was obtained in terms of the equilibrium surface energy and interplanar spacing of the planes perpendicular to the tensile axis and the appropriate Young's modulus.

An estimate of the theoretical shear strength was obtained from the shear modulus, the repeat distance of atoms in the direction of shear of the metal and interplanar spacing of the shearing planes.

The adhesion and friction properties of metals in contact with diamond, boron nitride, silicon carbide, manganese-zinc ferrite, and metals were examined in a vacuum of  $3 \times 10^{-8}$  pascal at low sliding speed. The coefficients of friction for clean metals in contact with these clean nonmetals and met-

als can be generally related to the theoretical tensile, theoretical shear and actual shear strengths of the metals. The higher the strength of the metal, the lower the coefficient of friction.

#### REFERENCES

1. Pauling, L., "A Resonating-Valence-Bond Theory of Metals and Intermetallic Compounds," Proc. Roy. Soc. (London), Ser. A, 196, 1046, 343-362, (Apr. 1949).
2. Buckley, D. H., "The Metal-to-Metal Interface and Its Effect on Adhesion and Friction," J. Colloid Interface Sci., 53, 1, 36-53, (Jan. 1977).
3. Miyoshi, K. and Buckley, D. H., "Adhesion and Friction of Single-Crystal Diamond in Contact with Transition Metals," Application of Surface Science, 6a, 161-172, (1980).
4. Buckley, D. H., "Friction and Transfer Behavior of Pyrolytic Boron Nitride in Contact with Various Metals," ASLE Trans., 21, 2, 118-124, (Apr. 1978).
5. Miyoshi, K. and Buckley, D. H., "Friction and Wear Behavior of Single-Crystal Silicon Carbide in Sliding Contact with Various Metals," ASLE Trans., 22, 3, 245-256, (July 1979).
6. Miyoshi, K. and Buckley, D. H., "Friction and Wear of Single-Crystal Manganese-Zinc Ferrite," Wear, 66, 2, 157-173, (1981).
7. Macmillan, N. H., "Review: The Theoretical Strength of Solids," J. Mater. Sci., 7, 2, 239-254, (Feb. 1972).
8. Bridgman, P. W., "Shearing Phenomena at High Pressures, Particularly in Inorganic Compounds," Proc. Am. Acad. Arts Sci., 71, 387-460, (1937).
9. Polanyi, M., "Über die Natur des Zerreibvorganges," Z. Physik., 7, 323-327, (1921).

10. Orowan, E., "Mechanical Cohesion Properties and the "Real" Structure of Crystals," Z. Kristallog., 89, 3-4, 327-343, (Oct. 1934).
11. Orowan, E., "Fracture and Strength of Solids," Rep. Prog. Phys., 12, 185-232, (1948-1949).
12. Orowan, E., "Energy Criteria of Fracture," Weld J., 34, 3, 1575-1605, (Mar. 1955).
13. Frenkel, J., "Zur Theorie der Elastizitätsgrenze und der Festigkeit Kristallinischer Körper," Z. Phys., 37, 7-8, 572-609, (1926).
14. Tyson, W. R., "Surface Energies of Solid Metals," Can. Metall. Q., 14, 4, 307-314, (1975).
15. Jones, H., "The Surface Energy of Solid Metals," Met. Sci. J., 5, 15-18, (Jan. 1971).
16. Murr, L. E., "Interfacial Phenomena in Metals and Alloys," Addison-Wesley Publ. Co., (1975).
17. Overbury, S. H., Bertrand, P. A., and Somorjai, G. A., "Surface Composition of Binary Systems; Prediction of Surface Phase Diagrams of Solid Solutions," Chem. Rev., 75, 5, 547-560, (1975).
18. Eustathopoulos, N., Joud, J. C., and Desre, P., "Interfacial Tension of Pure Metals. I--Estimation of the Liquid-Vapor and Solid-Vapor Surface Tensions From the Cohesion Energy. II--Estimation of the Solid-Vapor and Solid-Liquid Interfacial Tensions From the Surface Tension of Liquid Metals," J. Chim. Phys. Physicochim. Biol., 70, 1, 38-49, (1973).
19. Linford, R. G., "Surface Thermodynamics of Solids," Solid State Surface Science II, ed. by M. Green, Marcel Dekker, (1973), pp. 1-152.
20. Roth, T. A., "Surface and Grain-Boundary Energies of Iron, Cobalt and Nickel," Mater Sci. Eng., 18, 2, 183-192, (1975).

21. Miedema, A. R., "Surface Energies of Solid Metals," Z. Metallk., 69 5, 287-292, (May 1978).
22. Winterbottom, W. L., "Crystallographic Anisotropy in the Surface Energy of Solids," Surfaces and Interfaces, Vol. 1, Chemical and Physical Characteristics, ed. by J. J. Burke, N. L. Reed, and V. Weiss, Syracuse Univ. Press, (1967), pp. 133-165.
23. Tyson, W. R., Ayres, R. A., and Stein, D. F., "Anisotropy of Cleavage in bcc Transition Metals," Acta Met., 21, 5, 621-627, (May 1973).
24. Basterfield, J., Miller, W. A., and Weatherly, G. C., "Anisotropy of Interfacial Free Energy in Solid-Fluid and Solid-Solid Systems," Can. Metall. Quart., 8, 2, 131-144, (1969).
25. Gschneidner, K. A., Jr., "Physical Properties and Interrelations of Metallic and Semimetallic Elements," Solid State Physics, Vol. 16, ed. by F. Seitz and D. Turnbull, Academic Press, (1964), pp. 275-426.
26. Barrett, Charles Sanborn, Structure of Metals. Crystallographic Methods, Principles, and Data, McGraw-Hill Book Co., Inc., (1943), pp. 552-554.
27. Lyman, T., ed., Metals Handbook. Vol. 1: Properties and Selection of Metals, Eighth ed., American Society for Metals, (1961).
28. Tegart, W. J. M., Elements of Mechanical Metallurgy. Macmillan Co., (1966).
29. Timoshenko, S. and Goodier, J. N., Theory of Elasticity, Second ed., McGraw-Hill Book Co., (1951).

TABLE I. - VALUES FOR SURFACE ENERGY, YOUNG'S (ELASTIC) MODULUS, SHEAR MODULUS,  
LATTICE CONSTANTS AND SLIP SYSTEMS OF VARIOUS METALS

Metal	Structure	Estimated surface energy, $\text{mJ/m}^2$		Young's modulus, GPa	Shear modulus, GPa	Lattice constants, nm			Slip systems <sup>e</sup>	
		At room temperature, $\gamma$	At absolute zero, $\gamma_0$			a	c	Directions	Planes	
Al	bcc	1150	1200	71.0	27	0.405	—	—	<110>	{111}
Ni		2400	2450	193	75	.352	—	—		
Cu		1800	1850	126	45	.361	—	—		
Rh		2700	2750	372	150	.380	—	—		
Pd		2050	2100	123	51	.388	—	—		
Ir		3050	3100	527	210	.384	—	—		
Pt		2500	2550	171	61	.393	—	—		
V	bcc	2550	2600	131	47	0.304	—	—	<111>	{110} {112} {123}
Cr		2350	2400	243	117	.288	—	—		
Fe		2500	2550	210	81	.287	—	—		
Nb		2650	2700	105	37	.330	—	—		
Mo		2900	2950	327	116	.314	—	—		
Ta		3000	3050	181	69	.330	—	—		
W		3250	3300	397	150	.316	—	—		
Ti	hcp	2000	2050	106	39	0.295	0.468	—	<1120>	{0001}
Co		2500	2550	206	76	.251	.407	—	<1123>	{1010}
Y		1050	1100	64.8	26	.365	.573	—		{1011}
Zr		1900	1950	92.0	34	.323	.515	—		{1122}
Ru		3000	3050	412	160	.270	.428	—		
Re		3600	3650	461	180	.276	.446	—		

<sup>a</sup>From Miedema (ref. 21).

<sup>b</sup>face centered cubic.

<sup>c</sup>body centered cubic.

<sup>d</sup>Hexagonal close packed.

<sup>e</sup>At room temperature.

ORIGINAL PAGE IS  
OF POOR QUALITY

TABLE II. - SIMPLE CALCULATIONS OF THE THEORETICAL TENSILE STRENGTH

	$\sigma_{\max}$ , GPa	$\sigma_{\max}/E$	$\sigma_{\max}$ , GPa	$\sigma_{\max}/E$	$\sigma_{\max}$ , GPa	$\sigma_{\max}/E$
fcc	Tensile direction					
	<111>		<100>		<110>	
Al	19	0.27	20	0.28	24	0.34
Ni	48	.25	67	.35	68	.35
Cu	33	.26	47	.37	47	.37
Rh	68	.18	96	.26	97	.26
Pd	34	.28	47	.38	48	.39
Ir	85	.16	120	.23	122	.23
Pt	43	.25	61	.36	62	.36
bcc	Tensile direction					
	<110>		<100>		<111>	
V	39	0.30	47	0.36	62	0.47
Cr	53	.22	63	.26	83	.34
Fe	51	.24	60	.29	80	.38
Nb	35	.33	41	.39	54	.51
Mo	65	.20	78	.24	102	.31
Ta	48	.27	57	.31	75	.41
W	76	.19	90	.23	120	.30
hcp	Tensile direction					
	<0001>		<1120>		<1010>	
Ti	21	0.20	27	0.25	29	0.27
Co	36	.17	45	.22	49	.24
Y	11	.17	14	.22	15	.23
Zr	18	.20	23	.25	25	.27
Ru	54	.13	68	.17	73	.18
Re	61	.13	78	.17	83	.18

TABLE III. - VALUES OF COEFFICIENT OF FRICTION FOR VARIOUS  
PURE ELEMENTAL METALS IN CONTACT WITH DIAMOND,  
PYROLYTIC BORON NITRIDE, SILICON CARBIDE,  
Mn-Zn FERRITE AND THE METALS THEMSELVES

Metal	Coefficient of friction				
	Diamond	Pyrolytic boron nitride	Silicon carbide	Mn-Zn ferrite	Metals themselves
Al	----	----	0.60	----	----
Ni	0.48	0.72	.47	0.59	----
Cu	----	----	----	----	----
Rh	.37	.52	.36	.42	1.7
Pd	----	----	----	----	2.8
Ir	----	----	----	----	1.8
Pt	.50	.62	----	----	5.1
V	0.54	0.59	----	----	----
Cr	.43	----	0.48	----	10
Fe	.42	.46	.48	0.48	16
Nb	----	.64	----	----	----
Mo	----	----	----	----	5.1
Ta	----	.67	----	----	12
W	.42	----	.45	.50	----
Ti	0.72	1.0	0.58	0.83	60
Co	.47	----	.43	.55	----
Y	----	----	----	----	----
Zr	.70	.95	.53	----	40
Ru	----	.49	----	----	----
Re	.40	----	.39	----	----

TABLE IV. - METAL-TRANSFER TO SINGLE-CRYSTAL SILICON CARBIDE (0001)  
SURFACE AS A RESULT OF MULTIPLE PASS SLIDING

Form of metal transfer	Metals*										
	Al	Ti	Zr	Cu	Ni	Co	Cr	Fe	Re	Rh	W
Very small particle (submicron in size)	+	+	+	+	+	+	+	+	+	+	+
Piled-up particle (several microns in size)	+	+	+	+	+	+	+	+	-	-	-
Streak thin film	+	+	+	+	+	+	+	-	-	-	-
Multilayer film structure (piled up)	+	+	+	-	-	-	-	-	-	-	-
Lump particle (several microns in size)	(±)	(±)	(±)	-	-	-	-	-	+	+	+
Surface roughness of metal wear scar	← Rougher										
Chemical affinity of metal for silicon and carbon	Lesser →										
Resistance to shear and tear of metal	Greater →										

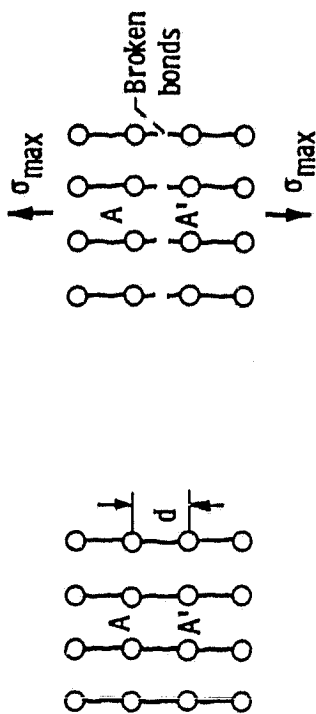
\*Transferred after 10 passes sliding +; not transferred after 10 passes sliding -; transferred after single pass sliding (+).

TABLE V. - SIMPLE CALCULATIONS OF THE

THEORETICAL SHEAR STRENGTH

(a)  $\Delta$  face-centered cubic structure; shear plane and direction,  $\{111\} \langle 110 \rangle$

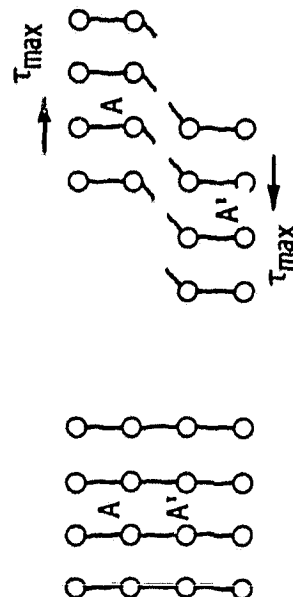
Metal	Shear strength, $\tau_{max}'$ GPa	Strength to modulus ratio, $\tau_{max}/G$
Al	2.6	0.096 - 0.098
Ni	7.3	
Cu	4.4	
Rh	15	
Pd	5.0	
Ir	21	
Pt	5.9	



(a) Tensile fracture.

(b) Body-centered cubic structure

Metal	Shear plane and direction					
	$\{110\} \langle 111 \rangle$		$\{112\} \langle 111 \rangle$		$\{123\} \langle 111 \rangle$	
	$\tau_{max}'$ GPa	$\tau_{max}/G$	$\tau_{max}'$ GPa	$\tau_{max}/G$	$\tau_{max}'$ GPa	$\tau_{max}/G$
V	3.1	0.065 - 0.66	5.3	0.11	8.1	0.17
Cr	7.6		13		20	
Fe	5.3		9.2		14	
Nb	2.4		4.2		6.4	
Mo	7.5		13		20	
Ta	4.5		7.8		12	
W	9.8		17		26	



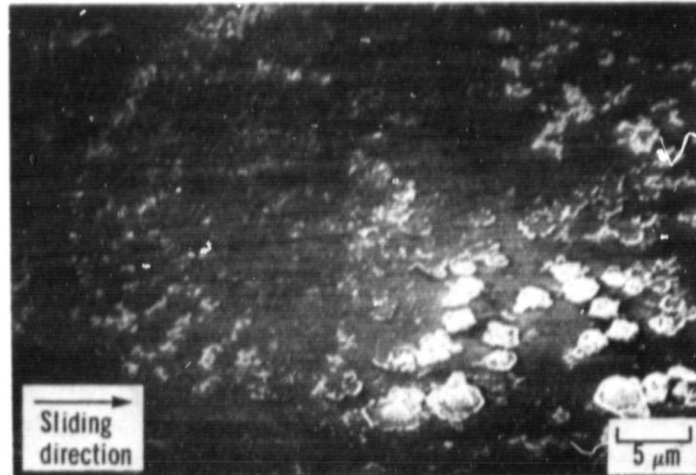
(b) Shear fracture.

(c) Hexagonal structure

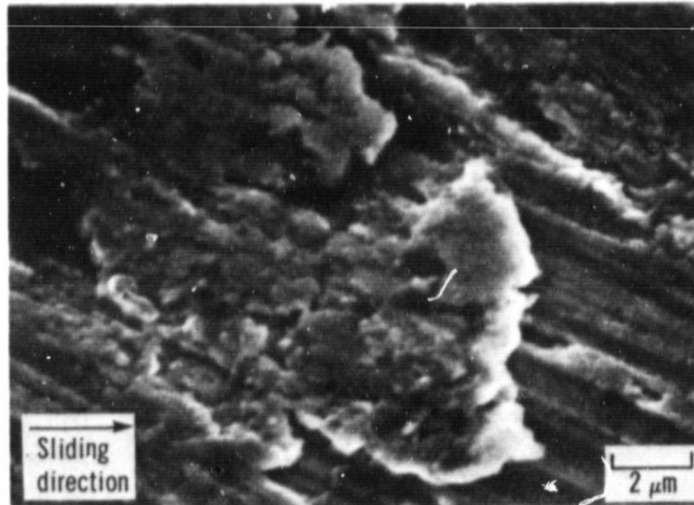
Metal	Shear plane and direction					
	$\{0001\} \langle 11\bar{2}0 \rangle$		$\{10\bar{1}0\} \langle 11\bar{2}0 \rangle$		$\{10\bar{1}1\} \langle 11\bar{2}0 \rangle$	
	$\tau_{max}'$ GPa	$\tau_{max}/G$	$\tau_{max}'$ GPa	$\tau_{max}/G$	$\tau_{max}'$ GPa	$\tau_{max}/G$
Ti	3.9	0.098 - 0.10	7.2	0.18 - 0.19	8.2	0.21
Co	7.5		14		16	
Y	2.6		4.8		5.5	
Zr	3.4		6.3		7.1	
Ru	16		29		34	
Re	18		33		38	

Figure 1. - Fracture viewed at atomistic level in terms of breaking of atomic bonds.

ORIGINAL PAGE  
BLACK AND WHITE PHOTOGRAPH



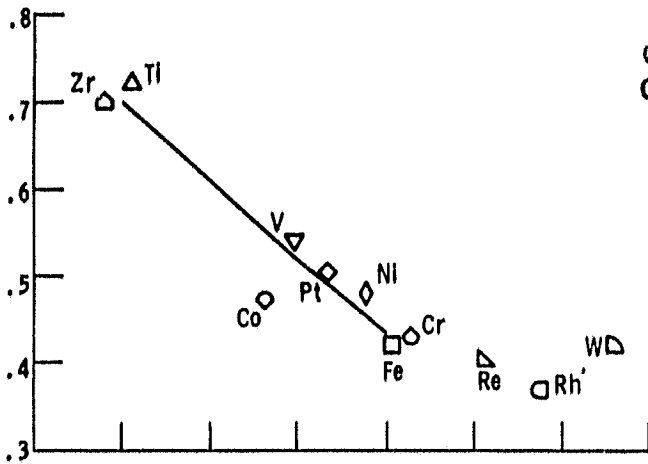
(a) Wear track showing transfer of iron to single-crystal silicon carbide.



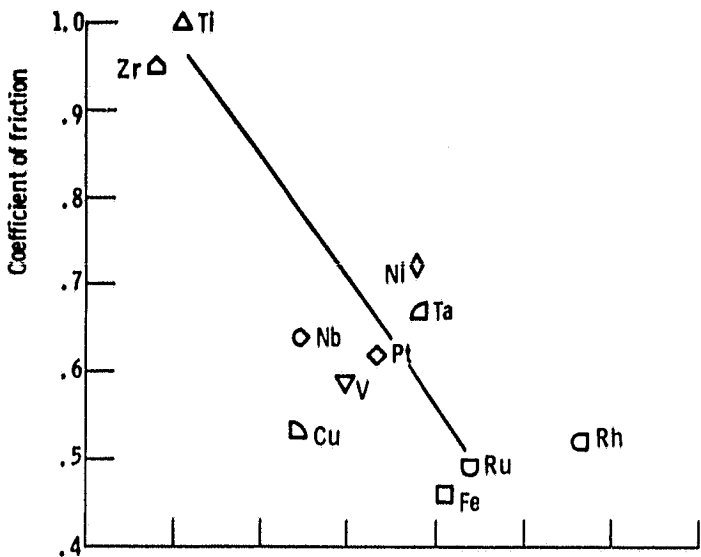
(b) Wear scar of iron.

Figure 2. - Scanning electron micrographs of wear track on the silicon carbide surface and wear scar of iron as a result of single pass of rider in vacuum. Silicon carbide  $\{0001\}$  surface; sliding direction  $\langle 10\bar{1}0 \rangle$ ; sliding velocity 3 mm/min; load, 0.2 N; room temperature; vacuum pressure,  $10^{-8}$  Pa.

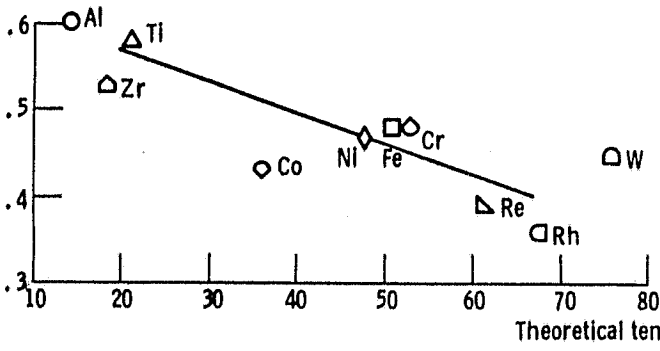
ORIGINAL PAGE IS  
OF POOR QUALITY



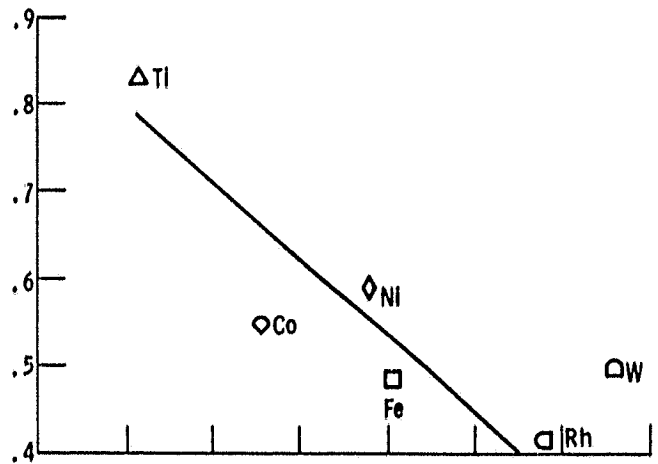
(a) Sliding material, single-crystal diamond (111) surface. Sliding direction,  $\langle 1\bar{1}0 \rangle$ ; sliding velocity, 3 mm/min; load, 0.05 to 0.3 N.



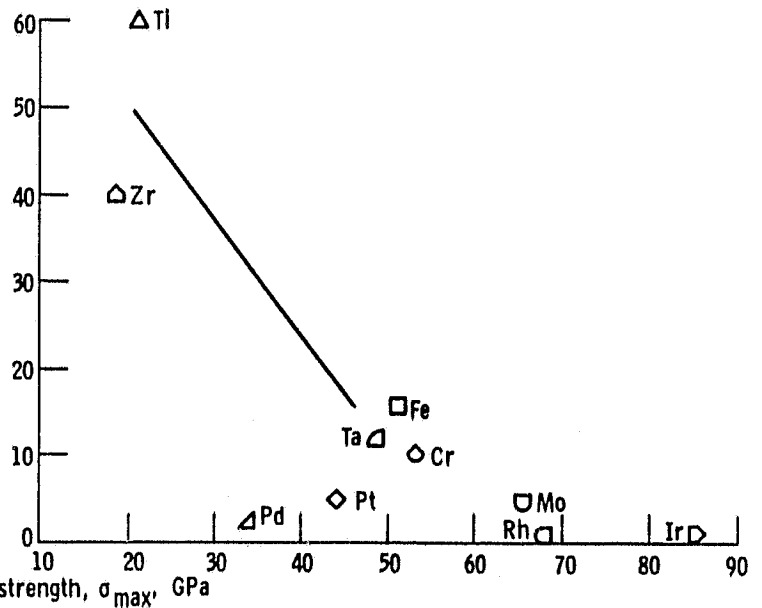
(b) Sliding material, pyrolytic boron nitride surface. Sliding velocity, 0.77 mm/min; load, 0.3 N.



(c) Sliding material, single-crystal silicon carbide (0001) surface. Sliding direction,  $\langle 10\bar{1}0 \rangle$ ; sliding velocity, 3 mm/min; load, 0.05 to 0.5 N.



(d) Sliding material, single-crystal manganese-zinc ferrite (110) surface. Sliding direction,  $\langle 1\bar{1}0 \rangle$ ; sliding velocity, 3 mm/min; load, 0.3 N.



(e) Sliding material, metals themselves. Sliding velocity, 0.7 mm/min; load, 0.01 N.

Figure 3. - Coefficients of friction as function of the theoretical tensile strength of metals in contact with nonmetals and themselves. Tensile direction:  $\langle 111 \rangle$  for fcc,  $\langle 110 \rangle$  for bcc, and  $\langle 0001 \rangle$  for hexagonal metals. Tests were conducted at room temperature at a vacuum pressure of  $10^{-8}$  Pa.

ORIGINAL PAGE IS  
OF POOR QUALITY

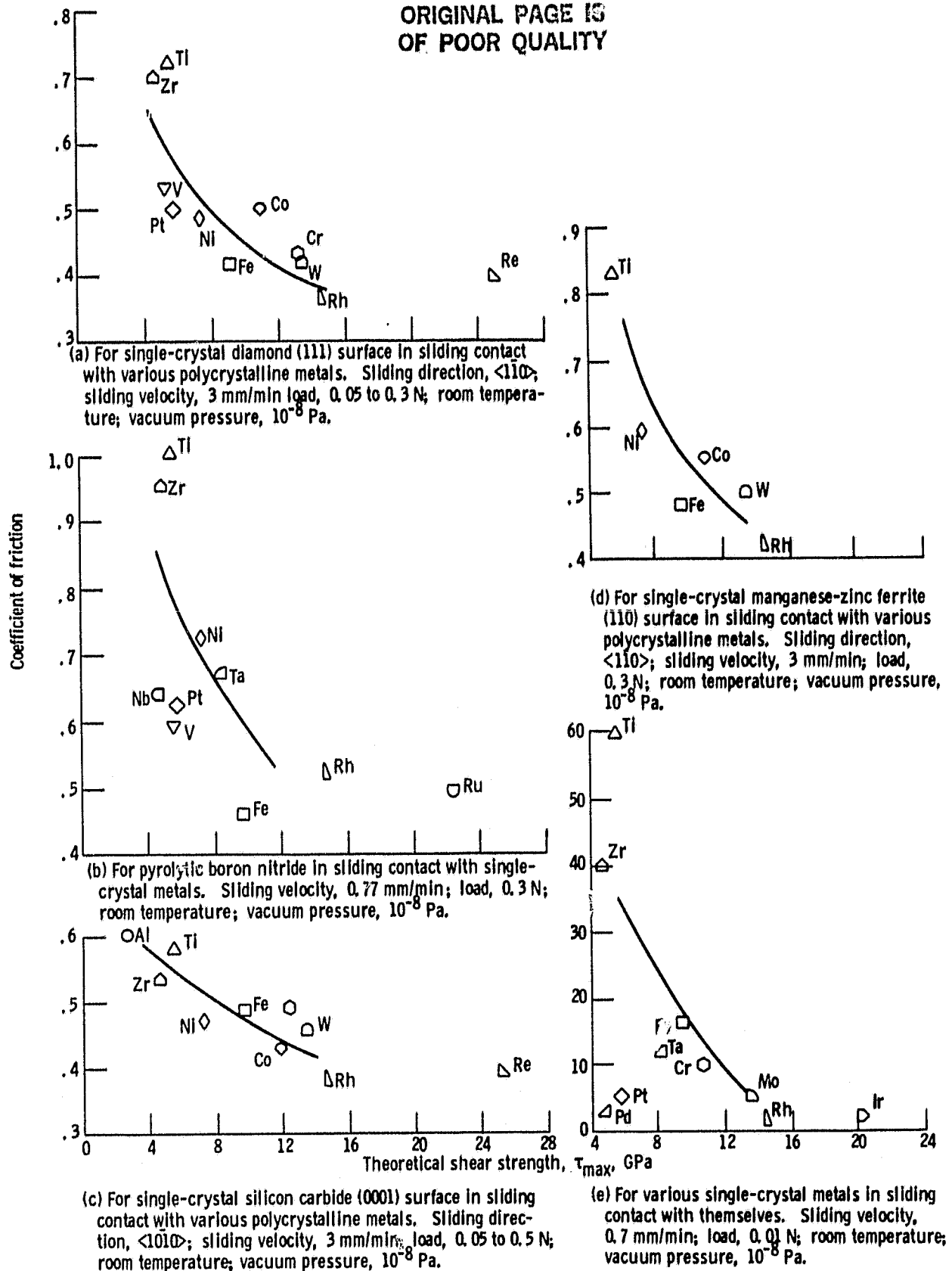
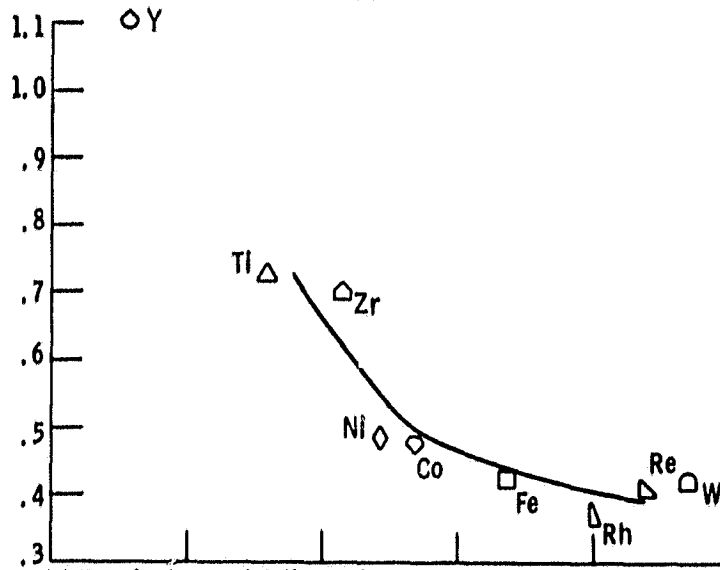
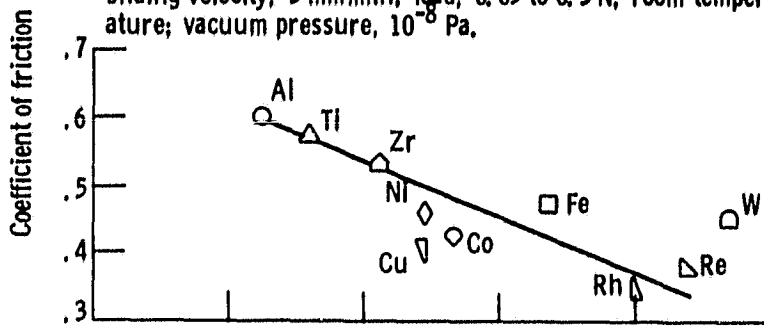


Figure 4. - Coefficients of friction as function of the theoretical shear strength of metals.

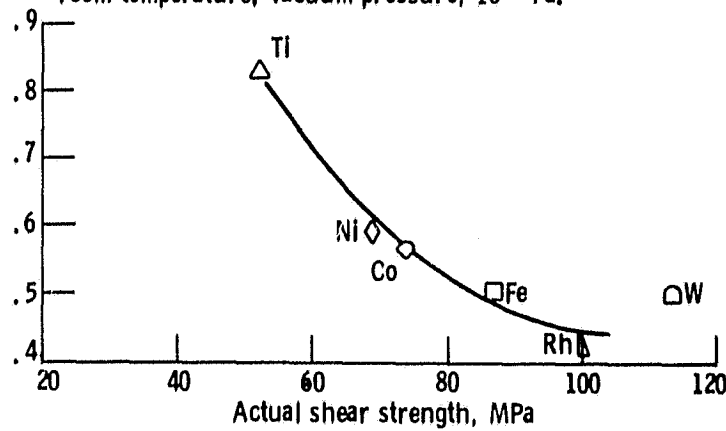
ORIGINAL PAGE IS  
OF POOR QUALITY



(a) For single-crystal diamond (111) surface in sliding contact with various polycrystalline metals. Sliding direction,  $\langle 1\bar{1}0 \rangle$ ; sliding velocity, 3 mm/min; load, 0.05 to 0.3 N; room temperature; vacuum pressure,  $10^{-8}$  Pa.



(b) For single-crystal silicon carbide (0001) surface in sliding contact with various polycrystalline metals. Sliding direction,  $\langle 10\bar{1}0 \rangle$ ; sliding velocity, 3 mm/min; load, 0.05 to 0.5 N; room temperature; vacuum pressure,  $10^{-8}$  Pa.



(c) For single-crystal manganese-zinc ferrite (110) surface in sliding contact with various polycrystalline metals. Sliding direction,  $\langle 1\bar{1}0 \rangle$ ; sliding velocity, 3 mm/min; load, 0.05 to 0.3 N; room temperature; vacuum pressure,  $10^{-8}$  Pa.

Figure 5. - Coefficients of friction as function of the actual shear strength of metals.